Contrib Mineral Petrol (2003) 146: 174–191
DOI 10.1007/s00410-003-0492-8

ORIGINAL PAPER

Timm John · Volker Schenk

Partial eclogitisation of gabbroic rocks in a late Precambrian subduction zone (Zambia): prograde metamorphism triggered by fluid infiltration

Received: 3 February 2003 / Accepted: 3 June 2003 / Published online: 19 July 2003

Abstract Gabbros and eclogites occur closely associated in a 200-km-long and up to 40-km-wide area of the Zambezi Belt in central Zambia. This area is interpreted to represent part of a late Precambrian suture zone, with the mafic rocks being relics of subducted oceanic crust. Gradual stages of prograde transformation from gabbro to eclogite are preserved by disequilibrium textures of incomplete reactions. This resulted in kyanite–omphacite-bearing assemblages for eclogites that have Al-poor bulk compositions. Undeformed eclogites typically preserve features of a former gabbroic texture, reflected by replacements of plagioclase and magmatic pyroxene by eclogite facies minerals. Textures of deformed eclogites range from sheared porphyroclastic to porphyroblastic. Relics of magmatic pyroxene are common and complete eclogitisation occurred only in millimetre to centimetre-scale domains in most of the rocks. No evidence for prograde blueschist or amphibolite facies mineral assemblages was found in eclogites. In contrast, the fine grained intergrowth of omphacite, garnet, kyanite and quartz, which replace former plagioclase or was formed in the pressure shadow of magmatic pyroxene relics, indicates that eclogitisation might have affected the gabbroic protoliths directly without any significant intervening metamorphic reactions. Eclogitisation took place under P–T conditions of 630–690 °C and 26–28 kbar, suggesting a large overstepping (> 10 kbar) of reaction boundaries. Eclogitisation was initialised and accompanied by a channelised fluid flow resulting in veins with large, subhedral grains of omphacite, kyanite and garnet. The gabbro-to-eclogite transformation was enhanced by a fluid which allowed the necessary material transport for the dissolution–precipitation mechanism that characterises the metamorphic mineral replacements. The process of eclogitisation was limited by reaction kinetics and dissolution–precipitation rates rather than by the metamorphic P–T conditions. Even though ductile deformation occurred and equilibrium phase boundaries were overstepped, the infiltration of fluids was necessary for triggering the gabbro-to-eclogite transformation.

Editorial responsibility: J. Hoefs

T. John (✉) · V. Schenk
Institut für Geowissenschaften and SFB 574,
Universität Kiel, 24098 Kiel, Germany
E-mail: tj@min.uni-kiel.de
Tel.: +49-431-8802864
Fax: +49-431-8804457

Introduction

The metamorphic transformation of the subducting slab governs several large-scale processes related to subduction zones. Devolatilisation of the slab triggers arc magmatism and the increasing density due to eclogitisation of the oceanic crust forces the lithospheric subsidence by slab pull. Rocks of the upper oceanic crust usually experience transformation into volatile-rich blueschists and subsequently into eclogites during burial. In contrast, the gabbroic part of the lower oceanic crust may transform directly to eclogites without intervening mineral reactions, as indicated by seismological and petrological data (e.g. Hacker 1996). Kirby et al. (1996), for example, explain intermediate depth earthquakes (50–170 km) in subduction zones with the volume reduction that accompanies the direct transformation from gabbro to eclogite. Yuan et al. (2000) imaged the subducting Nazca plate to a depth of about 120 km below the Andes where the crust became seismically invisible. They related this to the completion of the kinetically delayed gabbro-to-eclogite transformation. Disequilibrium textures of incomplete reactions, and metastabilities due to sluggish nucleation or slow diffusion rates and kinetics of reactions are commonly observed in rocks from low-T/high-P environments (Mørk 1985a, 1985b; Koons et al. 1987; Wayte et al. 1989; Rubie 1998; Engvik et al. 2001). Within dry, coarse-grained rocks, high pressure mineral assemblages

are sometimes formed only within fluid veins or in deformed domains. In such rocks, low-pressure minerals can persist metastably under conditions well above their equilibrium boundaries if no catalyst such as fluid triggers metamorphic reactions (e.g. Austrheim 1986/87; Hacker 1996; Rubie 1998; Austrheim 1998).

Central Zambia exhibits the largest number of Precambrian eclogite occurrences in Africa (Vrana et al. 1975). The eclogites and the associated gabbros (Fig. 1) are interpreted as relics of a fossil subducted slab that marks a suture zone between the Congo craton to the north and the Kalahari craton to the south. Similar isotopic and trace element compositions of the eclogites and gabbros show that they have a MORB-like bulk chemistry and, in combination with trace element ratios, it has been concluded that they are most likely co-genetic and were parts of the same subducted oceanic lithosphere (John et al. 2003a). Vrana et al. (1975) suggested that in addition to the P–T conditions, the fluid pressure and fluid composition, as well as the permeability of the rocks, were all crucial factors that controlled the transformation of gabbroic protoliths into eclogites. The Precambrian eclogites and gabbros of central Zambia provide an exceptional opportunity to study the fate of subducting oceanic gabbroic rocks. This paper describes the petrology of these eclogites and the transformation processes by which the gabbroic protoliths were eclogitised. These processes were predominantly fluid-controlled dissolution, transport and precipitation. Using textural and mineral chemical data, we deduce and document the important role of a fluid phase as a catalyst for eclogitisation, even in rocks that experienced pervasive deformation during metamorphism.

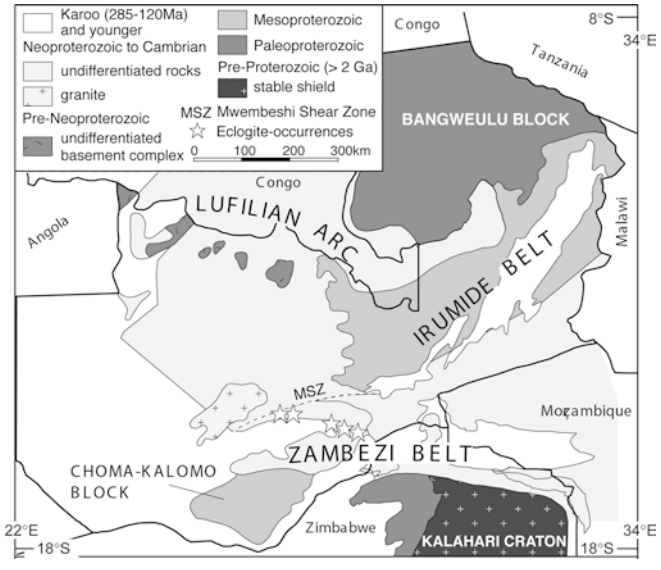

Fig. 1 Geological map (after Hanson et al. 1994; Sikatali et al 1994) showing structural provinces of Zambia and northern Zimbabwe. The northern margin of the Kalahari craton is shown while the southern margin of the Congo craton is north of this figure. Political borders have *thick lines*, while geological boundaries have *thin lines*. The eclogite-bearing zone is indicated by the *white stars*

Geological setting

The Precambrian orogens of Zambia consist of two major mobile belts (Fig. 1): (1) the Mesoproterozoic NE–SW striking Irumide Belt and Choma-Kalomo Block and (2) the Neoproterozoic to Cambrian Lufilian Arc and Zambezi Belt which are elongated in an E–W direction. The Irumide Belt formed during the assembly of Rodinia between 1.0 and1.3 Ga (e.g. Cahen et al. 1984; Hanson et al. 1988; Porada and Berhorst 2000), with the peak of ultra-high temperature metamorphism occurring at ca. 1.05 Ga (Schenk and Appel 2001).

The Zambezi Belt and the Lufilian Arc are part of the Pan-African orogenic system that crosscuts southern Africa, separating the Congo and Kalahari Cratons and their respective Paleo- and Mesoproterozoic units. These Pan-African belts were formed during the assembly of the Gondwana supercontinent. Eclogite facies metamorphism occurred at ca. 600 Ma (John et al. 2003a), whereas peak metamorphism during the subsequent continental collision occurred around 530 Ma ago, with metamorphic P–T conditions reaching the high pressure amphibolite facies (Goscombe et al. 1998, 2000; Vinyu et al. 1999; Johnson and Oliver 2002; John et al. 2003b). The Zambezi Belt crosscuts and thus divides the Mesoproterozoic parts of Zambia into the Irumide Belt and the Choma-Kalomo Block (Fig. 1). The junction of the Neoproterozoic belts and the Mesoproterozoic parts is marked by a 200-km-long and up to 40-km-wide zone containing lenses of eclogite, metagabbro, gabbro and rare ultramafic rocks (Fig. 2). The eclogite-bearing zone is located in the interior of the Zambezi Belt, and runs parallel to strike. The eclogites and associated mafic rocks form isolated hills of ten to a hundred metres in diameter. Neither contacts with the country rocks nor between the eclogites and the other mafic rocks are exposed. The country rocks consist mainly of kyanite-bearing metapelites, metapsammites and marbles (Fig. 2). Due to the strong weathering of metapelitic outcrops, useful petrological information about their metamorphic evolution is not preserved. The less altered marbles contain rare calc-silicate bands, but these lack critical mineral assemblages that could be used to determine the metamorphic evolution of the area. According to the tectonic model of Porada and Berhorst (2000), the mafic rocks of the Lufilian Arc–Zambezi Belt were incorporated into the platform and shelf sediments of the northern (i.e. the lower) plate during collisional overthrusting and backthrusting. This might explain the occurrence of isolated mafic blocks within the sedimentary country rocks. Porada and Berhorst (2000) proposed that during rifting, which is assumed to have started ca. 880 Ma ago, a passive continental margin was formed at the southern edge of the Congo craton. These authors pointed out that their depositional and tectonic model for the Lufilian Arc and northern Zambezi Belt requires the opening and closure of a major ocean. However, a geochemical study of gabbros and

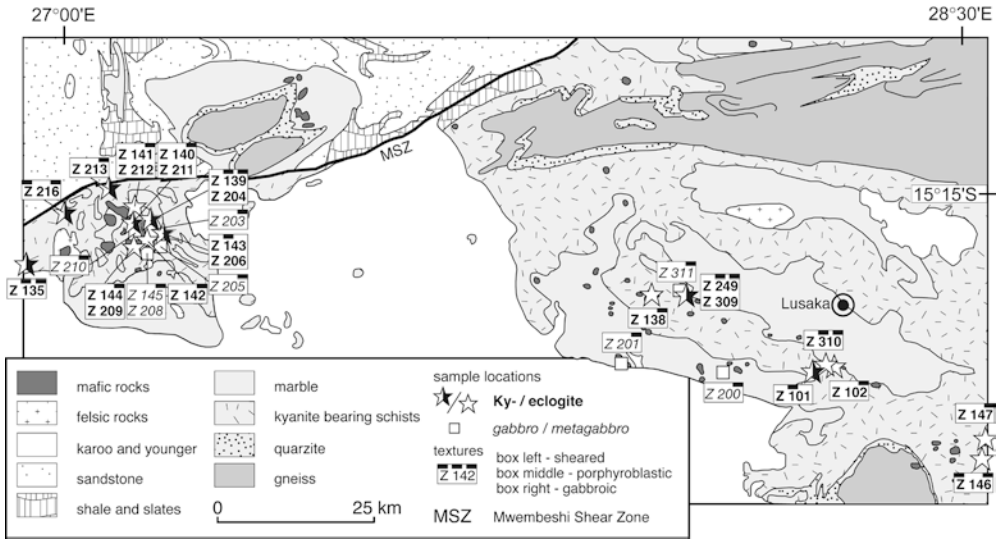

Fig. 2 Enlarged and simplified geological map of central Zambia after Thieme (1984) showing the sample locations. Eclogite occurrences are indicated by *stars* (*half black stars* Ky-bearing) and *bold sample numbers*; gabbro occurrences are indicated by *squares* and *italic sample numbers*. The *black boxes at the top of the sample-labels* indicate the observed textures in samples from the particular locality (see legend)

metagabbros from the Lufilian Arc suggested that the rifting in this region probably did not proceed beyond an intracontinental stage (Tembo et al. 1999). In contrast, geochemical data of gabbros and eclogites from central Zambia, which are considered here, imply that the parental magmas of these rocks formed at an oceanic spreading centre, and consequently it is argued that these rocks are relics of a subducted oceanic crust (John et al. 2003a).

Petrology

Eclogites were found at 16 of 23 investigated outcrops of mafic rocks, nine of which include Ky-bearing eclogites (Fig. 2). At 12 of the 23 localities, amphibolites, Grt–amphibolites and gabbros occur (Table 1). Even when eclogites and gabbros occur together in a single outcrop, contacts between them were not found. A typical feature of most of the Zambian eclogites is that they usually contain only small domains in which the complete transformation to eclogite has occurred. Partially eclogitised rocks with disequilibrium textures are more common than completely transformed and well-equilibrated ones. To simplify the description of the studied rocks, all samples that contain an eclogite facies mineral assemblage (i.e. omphacite and garnet), at least in subdomains, are called eclogites in this paper. Retrograde overprinting affected eclogite facies assemblages to varying, but mostly minor degrees; pervasive amphibolitisation is rare but a late-stage scapolitisation is found in many outcrops. The Zambian eclogites can be subdivided into three groups based on their dominant textures. The first group has a preserved gabbroic (i.e. igneous) texture, the second group has a porphyroblastic texture, and the third group has a sheared porphyroclastic texture. The textures of the eclogites are highly variable even at the thin section scale, with many outcrops displaying two of the textural types. The eclogitisation was accompanied by channelised fluid infiltration, which is visible in the form of veins with large omphacite, garnet, kyanite, and rare epidote crystals. Mineral relics of the magmatic protoliths are restricted to clinopyroxene. Plagioclase is not preserved, even in partially transformed rocks.

Table 1 Textures and rock types of investigated mafic rocks. Localities are shown in Fig. 2. Bold type indicates Ky-bearing rocks

Textures of eclogites			Non-eclogites
Gabbroic (Group 1)	Porphyroblastic (Group 2)	Sheared (Group 3)	Gabbro/ Metagabbro
Z 102	**Z 101**	Z 146[a]	Z 145/208
Z 135[a]	**Z 135**[a]	**Z 216**[a]	Z 200
Z 138[b]	**Z 139/204**	–	Z 201
Z 139/204	**Z 143/206**[b]	–	Z 203
Z 140/211	**Z 249**[b]	–	Z 205
Z 141/212	**Z 310**[ab]	–	Z 311
Z 142[b]	–	–	–
Z 144/209	–	–	–
Z 146[a]	–	–	–
Z 147[b]	–	–	–
Z 213	–	–	–
Z 216[a]	–	–	–
Z 310[ab]	–	–	–

[a]Magmatic relics
[b]With gabbro/metagabbro

Petrography

Group 1: eclogites with gabbroic textures

Eclogites that contain relics of a medium-grained gabbroic texture are common, occurring at 13 of the 16 eclogite localities (Fig. 2; Table 1). The former gabbroic texture is reflected by the shape of garnet which replaces plagioclase laths, and omphacite which

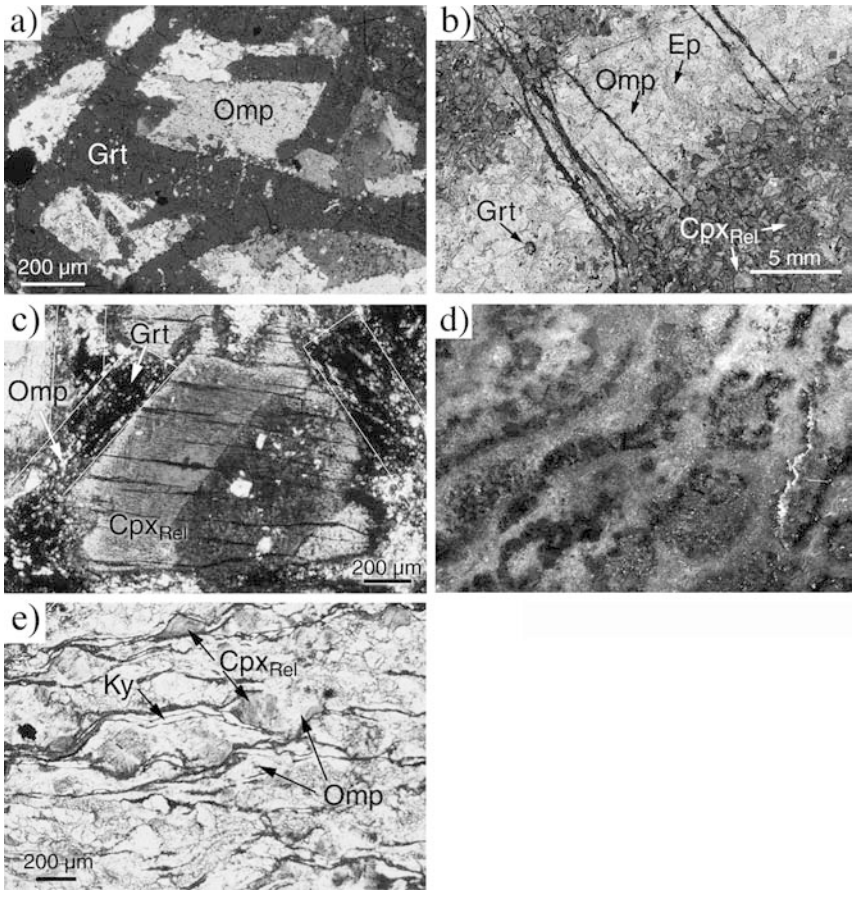

Fig. 3a Preserved gabbroic texture in an eclogite. Garnet forms pseudomorphs after plagioclase (*dark*) and omphacite replaces magmatic pyroxenes (*bright*). Note lack of strain fabric in the replacement assemblage (Z146–1). **b** A major fluid infiltration vein (*light*) in a partially eclogitised rock (Z310–4). The *darker* matrix consists of omphacite–garnet–kyanite–quartz symplectites between magmatic clinopyroxene relics. The vein consists of epidote-group minerals (*darker grey*), omphacite (*brighter grey*) composed of ca. 10 µm subgrains, and rare garnet. Thin, dark veins of greenschist facies minerals cut across the eclogite facies vein. **c** Relic of a magmatic pyroxene (Cpx_{Rel}) showing preserved magmatic twinning (enlarged from Fig. 3b). The bright patches within the crystal are late-stage hornblende. Plagioclase laths that once surrounded the magmatic pyroxene have been replaced by fine grained Grt (*dark*) + Cpx_{Omp} (*bright*) + quartz + kyanite intergrowths (*indicated by thin white outlines*). **d** Lens-like porphyroblastic eclogite (Z143–8). Garnet aggregates (*dark grey*) form lenses within an omphacitic matrix (*light grey*). Field of view ca. 4 cm. **e** Sheared eclogite (Z 216–7). Most omphacite (*white*) has grown in the pressure shadows of magmatic clinopyroxene relics (Cpx_{Rel}; *dark grey*). Thin bands of kyanite (*white*) surround the clinopyroxene porphyroclasts

replaces the magmatic, interstitial clinopyroxene (Fig. 3a). Magmatic clinopyroxene relics are common, and, in most cases, complete eclogitisation occurred only in millimetre-scale domains. In some samples a complete eclogitisation occurred only along vein-like fluid paths (Fig. 3b). These eclogites contain epidote-group minerals, which occur mainly in the matrix. In this case, the epidote-group minerals, instead of garnet, replace the plagioclase laths, and garnet is only a minor phase. Very fine grained quartz and kyanite typically occur within the matrix and as inclusions in garnet of the less eclogitised rocks. This kyanite is anhedral or forms tiny needles. The rims of the magmatic clinopyroxene relics are usually transformed to omphacite, whereas the cores of the grains have almost perfectly preserved magmatic compositions. Former plagioclase laths located close to clinopyroxene relics are pseudomorphically replaced by a fine grained intergrowth of anhedral garnet, omphacite, kyanite and quartz (Fig. 3c).

Group 2: eclogites with porphyroblastic textures

Eclogites with porphyroblastic textures were found at six localities (Fig. 2; Table 1). In some of them Grt-rich and Omp-rich zones may form lenses up to a few centimetres in length (Fig. 3d). Some of the omphacite crystals are oriented parallel to the lenses. The more porphyroblastic parts are characterised by large (up to 1 cm) garnet porphyroblasts in an omphacite matrix. These garnets are mostly ellipsoidal, and their rims are typically clouded with minute omphacite inclusions. Some garnets form large aggregates of anhedral porphyroblasts surrounding several garnet cores. The fine grained omphacitic matrix has mostly amoeboid grain boundaries. In some domains the omphacite crystals are coarser-grained due

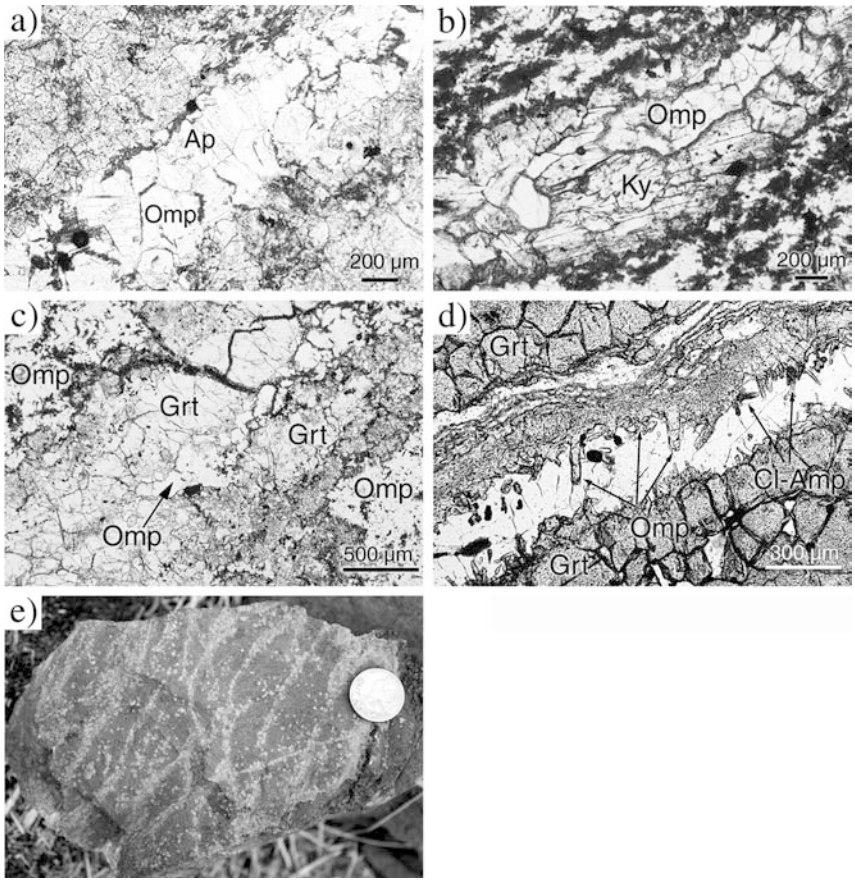

Fig. 4a Vein in eclogite consisting of large, subhedral omphacite and apatite crystals. The surrounding matrix consists of fine grained garnet and omphacite replacing the former magmatic texture (Z 146–2). **b** Vein consisting of kyanite and omphacite with preserved growth zoning. The vein follows the fabric of the host eclogite (Z143–8). **c** Garnet–omphacite vein in a porphyroblastic eclogite (Z 139–3). The vein consists of large omphacites in the centre surrounded by garnet. At the rim of the vein, the garnet is clouded with omphacite inclusions (*darker grey*). The rock matrix consists of omphacite. **d** Vein in a porphyroblastic eclogite (Z249–6). The vein consists of euhedral omphacites (grey) with preserved growth zoning, potassium-rich Cl-amphiboles (*dark*), garnet (*at the rim*), quartz (*white*), and apatite (not shown). At the upper part of the vein older mainly quartz filled cracks, formed during multiple opening of the vein, are shown. **e** Eclogite crosscut by mainly garnet-bearing veins of different orientations (locality Z 249)

to static recrystallisation and display equilibrium grain boundaries. No relics of magmatic textures or minerals are preserved in the group 2 eclogites.

Group 3: sheared porphyroclastic eclogites

Sheared eclogites were found at only two localities (Fig. 2; Table 1). Most of these rocks are partially sheared to varying extents, but a strong, pervasive deformation is rare. The eclogites contain porphyroclastic relics of magmatic clinopyroxene (Fig. 3e) and, as for the eclogites of the group 1, complete eclogitisation occurred only within millimetre-scale domains. The relics of magmatic clinopyroxenes and the garnets form s-parallel oriented and elongated porphyroclasts in a matrix of very fine grained (ca. 10 µm) omphacite, quartz and kyanite. The magmatic pyroxene relics have small omphacitic rims which increase in thickness towards one side of the grain. However, most omphacite grew within the pressure shadows and the fine grained matrix. Thin, millimetre-long bands of fine grained kyanite crystals follow the foliation and wrap around the clinopyroxene relics (Fig. 3e). Garnet typically occurs as subparallel oriented laths and, within the strongly sheared parts, as deformed porphyroclasts.

Eclogitic veins

Eclogitic veins occur in almost all investigated eclogites. They are composed of large (millimetre-scale) omphacite grains, which are sometimes associated with kyanite, garnet, or apatite (Fig. 4a, b). However, some veins consist mostly of garnet, with omphacite only occurring in the centres of these veins (Fig. 4c). Other veins contain garnet, omphacite, amphibole and kyanite. In these veins, omphacite and garnet are usually dilated and healed several times during multiple openings of the vein (crack and seal process; Fig. 4d). The veins are more or less randomly oriented (Fig. 4e), crosscutting the main fabric in most cases. They range in width from less than 1 mm to more than 1 cm. In rare cases, veins contain epidote-group minerals instead of garnet (Fig. 3b), associated with very fine grained (ca. 10 µm) omphacite.

Table 2 Mineral assemblages during the metamorphic evolution of the Zambian eclogites

Metamorphic stage	Mineral assemblages
Pre metamorphism	Pl + Cpx(mag) + Ilm
Peak: eclogitisation	Grt + Cpx(Omp) + Rt ± Ky ± Ep/Czo ± Qtz ± Phe ± Amp
Retro: amphibolitisation	Pl + Amp + Cpx(Di) + Qtz ± Grt ± Ep/Czo ± Scp

Mineral chemistry and growth history

Elemental analyses of minerals (Tables 3, 4, 5, 6) were performed on JEOL 8900 electron microprobes in Kiel and Göttingen, both equipped with five wavelength-dispersive spectrometers (WDS). For mineral analyses, these instruments were typically operated with a 15 kV acceleration voltage and a focused, 15 nA beam. Sample spot sizes were ca. 1 μm in diameter. Citzaf was used for the matrix correction of the raw counts. Both natural and synthetic mineral standards were used.

To illuminate the formation history of the eclogite facies assemblages (Table 2), the relevant mineral reactions will be introduced here. Only generalised, non-stoichiometric reactions are given (mineral abbreviations after Kretz 1983).

The plagioclase components convert to eclogite facies phases through reactions of the kind:

$$\mathrm{An} \Rightarrow \mathrm{Grs} + \mathrm{Ky} + \mathrm{Qtz} \quad (1)$$

$$\mathrm{An} + \mathrm{H_20} \Rightarrow \mathrm{Czo/Zo} + \mathrm{Ky} \quad (2)$$

$$\mathrm{Ab} \Rightarrow \mathrm{Jd} + \mathrm{Qtz} \quad (3)$$

These result in a near-isochemical plagioclase breakdown (Wayte et al. 1989):

$$\mathrm{Pl} \Rightarrow \mathrm{Grs} + \mathrm{Jd} + \mathrm{Ky} + \mathrm{Qtz} \quad \text{in a dry system, or} \quad (4)$$

$$\mathrm{Pl} + \mathrm{H_2O} \Rightarrow \mathrm{Czo/Zo} + \mathrm{Jd} + \mathrm{Ky} + \mathrm{Qtz} \text{ if } \mathrm{H_2O} \text{ is available.} \quad (5)$$

The augitic clinopyroxene ($\mathrm{Cpx_{Rel}}$) is converted to omphacite:

$$\mathrm{Aug} + \mathrm{Jd} \Rightarrow \mathrm{Omp} + (\mathrm{Ca, Fe, Mg})_2\mathrm{Si_2O_6} \quad (6)$$

while the excess Ca, Mg, Fe and Si of the augite are incorporated in garnet and epidote:

$$\left(\mathrm{Ca, Mg, Fe^{2+}}\right)_2\mathrm{Si_2O_6} + \mathrm{Ky} \Rightarrow \mathrm{Grs} + \mathrm{Pyr} + \mathrm{Alm} \quad (7)$$

$$\mathrm{Ca, Fe^{3+}} + \mathrm{Ky} + \mathrm{H_2O} \Rightarrow \mathrm{Ep}. \quad (8)$$

During retrograde metamorphism, the eclogites were partially transformed to amphibolite according to a reaction of the type:

$$\mathrm{Omp} + \mathrm{Grt} + \mathrm{H_2O} \Rightarrow \mathrm{Prg} + \mathrm{Pl} + \mathrm{Qtz} \pm \mathrm{Czo/Ep}, \quad (9)$$

where the plagioclase is usually replaced by scapolite.

Garnet

Garnet occurs as ellipsoidal porphyroblasts as well as pseudomorphic laths after plagioclase. Growth zoning of porphyroblastic garnet, characterised by an increase of the pyrope content towards the rim and an almandine- and sometimes spessartine-rich core, is preserved in almost all samples (Table 3). The X_{Fe}-value varies from sample to sample (X_{Fe} = 0.53–0.78), and generally decreases towards the rims. If garnet is zoned in

Table 3 Representative garnet analyses and structural formulae. Structural formulae on a basis of 12 oxygens

Sample	Z 101–5	Z 101–7	Z 101–11	Z 135–6	Z 139–3	Z 139–7	Z 143–8	Z 146–1	Z 216–5	Z 249–6	Z310–4a
Analyses	grt2.78	grx1.24	grx1p24	grt1–1.5	grt2.3	grt1.5b	grt1.2	grt2.14	ogo1 g.21	grx1.94	grt6.4
Location	Rim	Rim	Core	Rim	Rim	Rim	Rim	Rim	Rim	rim	rim
SiO_2	39.71	39.63	37.87	39.44	38.97	38.47	39.53	38.87	39.17	39.01	39.19
Al_2O_3	22.42	22.31	21.63	22.54	22.05	21.26	22.24	21.98	22.00	22.14	22.46
FeO	20.97	18.57	25.33	20.28	25.24	26.56	22.35	21.23	21.48	24.45	20.01
MgO	9.06	9.11	3.42	9.29	7.58	3.98	8.99	7.41	6.66	6.73	6.70
MnO	0.41	0.40	2.61	0.33	0.36	0.57	0.26	0.45	0.42	0.23	0.46
CaO	7.81	9.73	8.90	8.62	5.88	9.74	7.14	9.65	10.49	8.21	11.61
Total	100.38	99.75	99.76	100.50	100.08	100.58	100.51	99.59	100.22	100.77	100.43
Si	2.999	2.994	2.986	2.976	2.999	3.006	2.996	2.987	2.999	2.987	2.983
Al	1.995	1.987	2.010	2.004	2.000	1.958	1.987	1.992	1.985	1.998	2.015
Fe	1.324	1.173	1.670	1.280	1.625	1.736	1.417	1.364	1.375	1.566	1.274
Mg	1.020	1.026	0.402	1.045	0.870	0.464	1.016	0.849	0.760	0.768	0.761
Mn	0.026	0.026	0.174	0.021	0.023	0.038	0.016	0.029	0.027	0.015	0.030
Ca	0.632	0.788	0.752	0.697	0.485	0.816	0.580	0.795	0.860	0.673	0.947
Total	7.997	7.994	7.995	8.022	8.002	8.015	8.012	8.016	8.006	8.005	8.010
Alm	44	39	56	42	54	57	47	45	45	52	42
Grs	21	26	25	23	16	27	19	26	28	22	31
Pyr	34	34	13	34	29	15	34	28	25	25	25
Spes	1	1	6	1	1	1	1	1	1	0	1
XFe	0.56	0.53	0.81	0.55	0.65	0.79	0.58	0.62	0.64	0.67	0.63

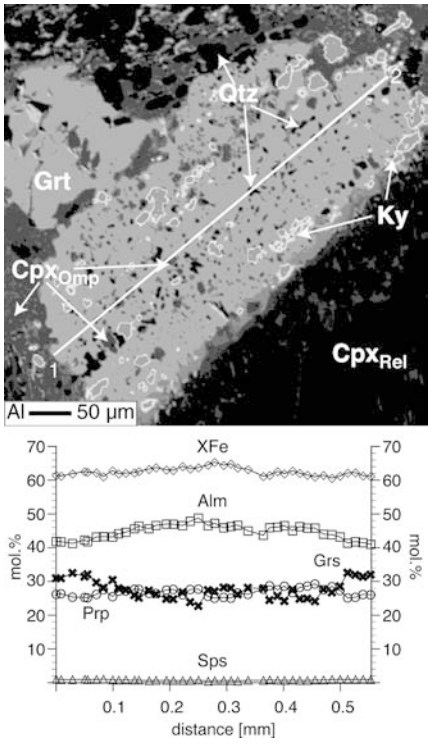

Fig. 5 Aluminium element mapping and chemical profile of a garnet which is part of the plagioclase replacement assemblage (see text). The garnet grew next to a magmatic pyroxene relic (Cpx_{Rel}) and shows a preserved growth zoning (X_{Fe} decreases and Grs-content increases towards the rim). The garnet (*light grey*) is lath-shaped and is intergrown with quartz (*black*), omphacite (Cpx_{Omp}, *dark grey*) and kyanite (*grey with white rim*). The intergrowth indicates that the garnet grew under eclogite facies conditions. The magmatic relic (Cpx_{Rel}) is also shown in Figs. 3b, 7b

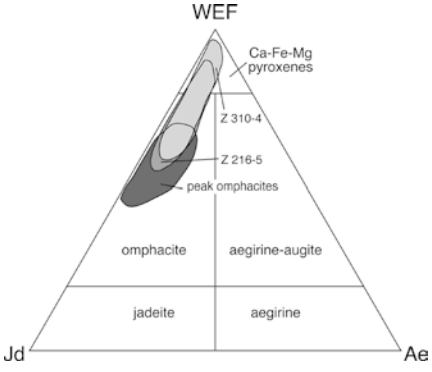

Fig. 6 Compositional ranges of pyroxenes (nomenclature after Morimoto et al. 1988), including the compositions of magmatic relics, from a sheared eclogite (Z 216–5) and an eclogite with relic gabbroic texture (Z 310–4). The peak omphacite compositions of several Zambian samples are also shown (Table 3)

grossular content, it increases rimwards. The zoning pattern indicates that garnet grew during increasing temperatures and, in cases of a rimward grossular increase, during a simultaneous increase in pressure. Garnet grown in veins often shows the same chemical zoning as the porphyroblastic matrix garnet. In some cases, garnet is intergrown with omphacite, kyanite and quartz, replacing former plagioclase laths (Fig. 5). This intergrowth is related to reactions (4), (6) and (7). In general, quartz inclusions are randomly distributed, whereas most kyanite and omphacite inclusions occur in the outer parts of the pseudomorphic garnet-laths (Fig. 5). This inclusion pattern points to garnet growth, or at least continued growth under eclogite facies conditions. Other inclusions are rutile and, rarely, epidote-group minerals and phengite. At locality Z 101, a second generation of garnet grew at lower pressure and temperature conditions. This garnet (Grt2) is only slightly zoned with a retrograde zoning at the rim. Grt2 has lower almandine(38–40) and grossular(12–21) and higher pyrope(37–48) components as compared to the rim compositions of prograde garnet [Grt1 = almandine(38–45), grossular(21–35), pyrope(32–34)].

Clinopyroxene

Omphacite usually has amoeboid grain boundaries. Polygonal textures with straight grain boundaries are rare, mostly occurring in veins and in group 2 eclogites. Different stages of the transformation from magmatic pyroxene to omphacite are preserved (Fig. 6; Table 4). The sheared porphyroclastic eclogites (group 3) contain magmatic pyroxene relics of diopsidic composition ($Wo_{49}Cfs_{43}Cen_8$_Jd_{10}; Table 4). The Jd-content of these pyroxenes increases considerably towards the rims (Jd_{10} to Jd_{35}). The compositional gradient is less pronounced on the side of a grain that underwent pressure solution, whereas towards the pressure shadow, the transition from diopside to omphacite is sharp (Fig. 7a). Since these pressure shadows contain only eclogite facies minerals formed through reactions (4), (6) and (7), it indicates that ductile deformation, as well as the metamorphic reactions, started under eclogite facies conditions. The conversion of magmatic pyroxene of the group 1 rocks (relict gabbroic texture) to omphacite is seldom complete. Their compositions normally range between Jd_{10} and Jd_{25}, and some grains contain unaffected domains with augitic compositions of ca. $Wo_{43}Cfs_{49}Cen_8$_Jd_2 (Figs. 3c, 7b). In most samples, the rims of the magmatic pyroxenes have been strongly affected by metamorphic reactions, as indicated by the corroded grain boundaries and a sudden increase in Jd-content (Fig. 7b). Omphacite that is part of the plagioclase replacing assemblage (Figs. 5, 7b) was formed mainly by reactions (4) and (6). Within these small-scale subsystems, omphacite has Jd-contents of 35–45 mol% (e.g. Cpx_{Omp} in Fig. 7b). Omphacite that formed along grain boundaries and cracks also contains 35–45 mol% jadeite. Peak-stage omphacite in the matrix of well-equilibrated eclogites (usually from group 2), as well as vein omphacites have 40–50 mol% jadeite (Fig. 6). They cannot be distinguished chemically from matrix omphacites in terms of Jd-content. Vein omphacites typically show zoning with increasing Jd-contents and X_{Fe}-values towards their rims. The formation of the

Table 4 Representative pyroxene analyses and structural formulae. Structural formulae on a basis of 6 oxygens. *n.d.* not detected

Sample Analysis Location	Z 101–5 cpxZ1.23 Rim	Z 101–7 cpxX1.2 Rim	Z 101–11 cpxX1p4 Core	Z 135–6 grt1omp1.1 Rim	Z 139–3 omp4.2 Rim	Z 139–7 pyx1.4 Rim	Z 143–8 omp2.6 Rim	Z 146–1 omp4.5 Rim	Z 216–5 ogo1.1 Rim	Z 216–5 cpx5L.53 Core of relic	Z 249–6 pyx7.11 Rim	Z 310–4 cpx1.4 Rim	Z 310–4a cpx1L.64 Core of relic
SiO_2	55.65	55.78	55.53	55.35	56.19	56.52	56.30	54.58	56.29	52.86	56.47	55.59	54.16
TiO_2	0.05	0.06	0.06	0.00	0.04	0.03	0.05	0.09	0.02	0.66	0.12	0.05	0.19
Al_2O_3	10.32	10.34	10.01	8.48	10.99	10.18	11.03	7.98	10.14	2.87	9.69	9.01	2.33
FeO	4.60	4.01	4.74	3.12	5.14	6.17	3.26	4.12	3.25	4.50	5.14	3.85	4.75
MgO	8.66	9.04	8.64	10.71	7.81	7.86	8.96	11.00	9.20	14.03	8.84	10.14	17.16
MnO	0.01	0.02	0.05	0.07	0.03	0.01	0.04	0.00	0.00	0.12	0.03	0.01	0.17
CaO	12.94	13.51	13.05	16.28	12.40	12.37	13.43	17.07	14.44	22.63	14.22	16.82	20.81
Na_2O	6.93	6.64	7.02	5.10	7.55	7.17	6.93	4.44	6.61	1.41	6.53	5.18	0.29
K_2O	0.00	0.00	0.01	0.00	0.00	0.00	0.00	0.00	0.00	0.00	0.01	0.00	0.00
Total	99.16	99.40	99.11	99.11	100.14	100.31	100.00	99.28	99.95	99.08	101.05	100.64	99.86
T_Si	1.989	1.989	1.986	1.989	1.988	2.008	1.988	1.971	1.993	1.947	1.992	1.974	1.974
T_Al	0.011	0.011	0.014	0.011	0.012	0.000	0.012	0.029	0.007	0.053	0.008	0.026	0.026
M1_Al	0.423	0.423	0.407	0.348	0.446	0.426	0.447	0.310	0.416	0.071	0.395	0.351	0.074
M1_Ti	0.001	0.002	0.002	0.000	0.001	0.001	0.001	0.002	0.001	0.018	0.003	0.001	0.005
M1_Fe^{3+}	0.064	0.043	0.089	0.017	0.080	0.049	0.036	0.024	0.042	0.000	0.053	0.028	0.000
M1_Fe^{2+}	0.050	0.052	0.041	0.061	0.061	0.108	0.045	0.071	0.054	0.136	0.085	0.083	0.000
M1_Mg	0.461	0.480	0.461	0.574	0.412	0.416	0.472	0.592	0.486	0.770	0.465	0.537	0.915
M2_Mg	0.000	0.000	0.000	0.000	0.000	0.000	0.000	0.000	0.000	0.000	0.000	0.000	0.017
M2_Fe^{2+}	0.024	0.024	0.011	0.016	0.011	0.026	0.016	0.029	0.000	0.003	0.014	0.003	0.145
M2_Mn	0.000	0.001	0.002	0.002	0.001	0.000	0.001	0.000	0.000	0.004	0.001	0.000	0.005
M2_Ca	0.496	0.516	0.500	0.627	0.470	0.471	0.508	0.660	0.548	0.893	0.537	0.640	0.813
M2_Na	0.480	0.459	0.487	0.355	0.518	0.494	0.475	0.311	0.454	0.101	0.447	0.357	0.021
M2_K	0.000	0.000	0.000	0.000	0.000	0.000	0.000	0.000	0.000	0.000	0.000	0.000	0.000
Total	4.000	4.000	4.000	4.000	4.000	4.000	4.000	4.000	4.000	3.996	4.000	4.000	3.995
Wo	45	46	45	48	45	44	47	48	48	49	47	50	43
Clino-En	42	43	42	44	40	39	44	43	43	43	40	42	49
Clino-Fs	13	11	13	7	15	17	9	9	9	8	13	9	8
WEF	52	54	51	64	48	51	52	69	55	90	55	64	98
Jd	42	42	40	34	44	44	44	29	41	10	39	33	2
Ae	6	4	9	2	8	5	4	2	4	0	5	3	0
XFe[a]	0.12	0.14	0.09	0.12	0.15	0.24	0.11	0.14	0.10	n.d.	0.18	0.14	n.d.
XFe[b]	0.23	0.20	0.24	0.14	0.27	0.31	0.17	0.17	0.17	0.15	0.25	0.17	0.13
Fe^{3+}/Fe^{total}	0.46	0.36	0.63	0.18	0.53	0.27	0.37	0.19	0.44	n.d.	0.35	0.25	n.d.

[a]Included Fe^{3+} calculation (charge balance)
[b]Fe^{2+} as Fe^{total}

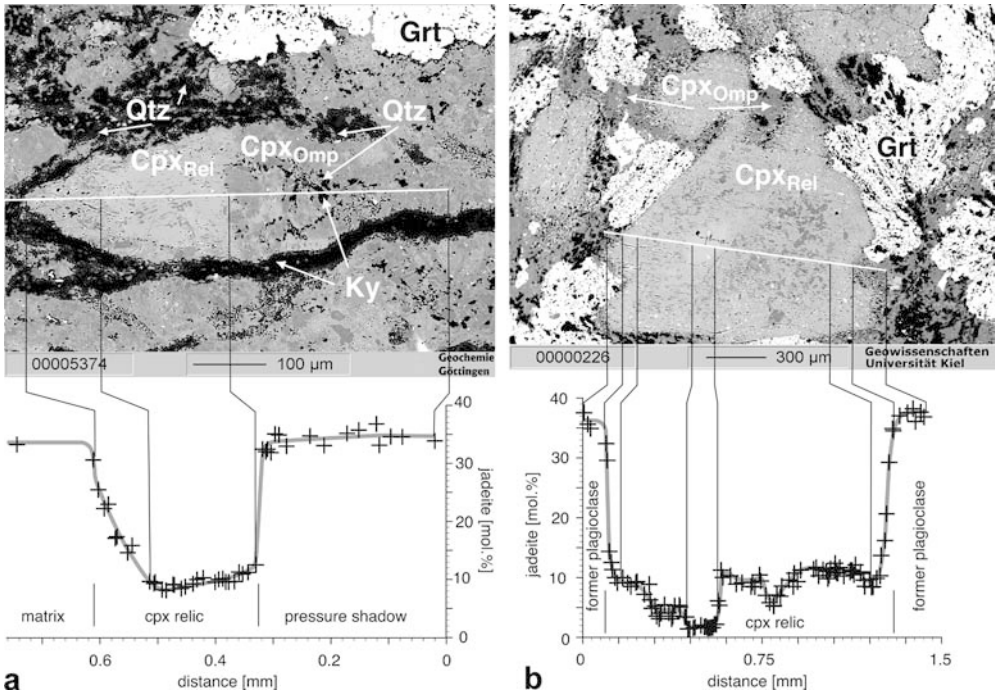

Fig. 7 **a** Back-scattered electron (BSE) image and chemical profile of clinopyroxene in a sheared eclogite that has magmatic relics (Z 216–5). Following the profile *from the left*, it starts in the matrix (not shown) with ca. 35 mol% jadeite, crosses a kyanite band (*black*), and enters the magmatic relic (Cpx_{Rel}). At this side of the grain, there is smooth transition from Jd_{35} at the rim to Jd_{10} in the core. In contrast, the boundary between the magmatic pyroxene relic and the omphacite (*dark grey*) in the pressure shadow is marked by a sharp compositional transition. The mineral assemblage in the pressure shadow is omphacite, quartz and kyanite; **b** BSE image and chemical profile of a magmatic pyroxene relic (Cpx_{Rel}) in an undeformed eclogite (same grain as in Fig. 3b; Z 310–4). Garnet (*white*), omphacite (Cpx_{Omp}, *dark grey*) with 35–40 mol% jadeite, kyanite (*black*) and quartz (*black*) have replaced plagioclase, while the augite was replaced by low-jadeite omphacite (Cpx_{Rel}, Jd_{10}, *bright grey*). Since kyanite and quartz are randomly distributed throughout the replacement they are not indicated separately. Note that only a thin rim of the Cpx_{Rel} shows a sharp increase of the jadeite content towards the matrix (see bright rim in Fig. 3b) and one area has an almost unaffected (magmatic) composition. The *dark grey patches* within Cpx_{Rel} are hornblende

Jd-content of ca. 10 mol% in the core of some magmatic relics (Cpx_{Rel} in Fig. 7a, b) is not well understood. One possible interpretation is that the Jd-content resulted from retrograde processes. The replacement of magmatic pyroxene by Jd_{10} pyroxene and amphibole may have taken place in crystals in which a fluid entered along cleavage planes. During retrogression, amphiboles grew within the widened cleavage planes and equilibrated with low jadeite pyroxenes within this subdomain under lower P–T conditions (Fig. 7a, b). Another possible explanation is that the inner part of the relic represented a subdomain during prograde fluid infiltration and associated replacement, which only slightly changed its composition due to limited transport of Na into the magmatic pyroxene grain. However, a common feature of the retrogression is the replacement of high-Jd omphacite by clinopyroxene symplectites that have lower and variable jadeite contents (10–30 mol%) or by quartz ± albite ± diopside ± amphibole intergrowths.

Amphibole

Edenitic to pargasitic amphiboles usually grew during the retrograde evolution of the rocks. They are found in omphacite-replacing symplectites, in coronas surrounding garnet, or as euhedral grains in the matrix. Rarely, hornblende occurs as inclusions in magmatic pyroxene relics. Hornblende most likely in textural equilibrium with prograde omphacite was found at one locality (Z 249) and is in this case interpreted as being formed under eclogite facies conditions. Hornblendes usually contain significant amounts of chlorine, ranging from 0.5 up to 5.8 wt%. These chlorine contents are positively correlated with potassium contents (e.g. a chlorine content of about 5–6 wt% is associated with a potassium content of up to about 3.3 wt%; Table 5). The unusual chlorine-rich amphiboles typically occur as vein-forming minerals (Fig. 4d; locality Z 249).

Epidote-group minerals

Minerals of the epidote group usually occur as anhedral grains grown at the rims of former plagioclase grains. In this case, they may have been part of the prograde plagioclase replacement assemblage or they may have partially replaced garnet during retrogression. Prograde epidote-group minerals also occur in veins as subhedral to anhedral grains consisting some-

Table 5 Representative analyses of chlorine-rich amphiboles from locality Z 249 and of retrograde hornblende from locality Z 101. Structural formulae on a basis of 24 oxygens, calculated after Leake et al. (1997); n.d. not detected

Sample	Z 249–6	Z 249–6	Z 101–5	Z 101–7	Z 101–11
Analysis	amp1.3	amp4.4	amp1p2	amp4p1	amp7p1
Location	Core	Rim	Rim	Rim	Rim
SiO_2	38.67	38.11	49.77	47.36	49.01
Al_2O_3	14.46	15.45	9.40	13.27	12.34
TiO_2	0.35	0.44	0.19	0.32	0.27
FeO	19.57	19.41	7.37	7.74	6.99
MgO	6.42	6.35	16.48	14.92	15.08
MnO	0.00	0.01	0.03	0.00	0.06
CaO	10.31	10.53	9.91	10.64	8.20
Na_2O	1.83	1.65	2.63	2.94	4.23
K_2O	3.23	3.31	0.65	1.08	0.61
H_2O-	0.41	0.44	1.98	2.00	2.00
F-	n.d.	n.d.	n.d.	n.d	n.d
Cl-	5.78	5.71	0.45	n.d	n.d
Total	101.03	101.41	97.33	100.27	98.79
Total cor.	99.73	100.12	97.23	100.27	98.79
Si	6.166	6.049	7.120	6.726	6.978
Al IV	1.834	1.951	0.880	1.274	1.022
Sum_T	8.000	8.000	8.000	8.000	8.000
Al VI	0.883	0.940	0.705	0.947	1.049
Ti	0.042	0.053	0.021	0.034	0.029
Mg	1.526	1.503	3.515	3.159	3.201
Fe^{2+}	2.549	2.505	0.760	0.859	0.722
Mn	0.000	0.000	0.000	0.000	0.000
Sum_C	5.000	5.000	5.000	5.000	5.000
Fe^{2+}	0.061	0.072	0.122	0.060	0.111
Mn	0.000	0.001	0.004	0.000	0.007
Mg	0.000	0.000	0.000	0.000	0.000
Ca	1.761	1.791	1.519	1.619	1.251
Na	0.178	0.136	0.356	0.321	0.631
Sum_B	2.000	2.000	2.000	2.000	2.000
Ca	0.000	0.000	0.000	0.000	0.000
Na	0.388	0.372	0.374	0.489	0.536
K	0.657	0.670	0.118	0.196	0.111
Sum_A	1.045	1.042	0.491	0.684	0.647
Sum_Tot	16.045	16.042	15.491	15.684	15.647
OH	0.438	0.464	1.890	1.895	1.899
F	0.000	0.000	0.000	0.000	0.000
Cl	1.562	1.536	0.109	0.000	0.000

times of very fine subgrains (ca. 10 μm), or as rare inclusions in garnets that seem to have replaced plagioclase. Pistacite content is not uniform, ranging between 0.3 and 0.6 mol%. No chlorine was detected in the epidote-group minerals.

Phengite

Phengites were found only in samples of locality Z 101 (Table 6), where they occur either in the matrix as part of the peak assemblage, or as inclusions in garnet. The phengite inclusions occur exclusively in rocks without matrix phengite. Si-contents of matrix phengite range between 3.34 and 3.46 pfu, with X_{Fe}-values between 0.12 and 0.19, whereas enclosed phengite has lower Si-contents between 3.20 and 3.36 pfu and higher X_{Fe}-values between 0.20 and 0.34. Their textural occurrence and lower Si-contents indicate that phengite inclusions probably formed during the prograde evolution. These prograde phengite inclusions have somewhat lower chlorine contents (ca. 0.1 wt%) than the matrix phengites (>0.2 wt%).

P–T conditions and phase relations

Peak metamorphic mineral assemblages are omphacite–garnet–rutile ± kyanite with rare quartz and epidote-group minerals in the matrix and as inclusions in garnet. Temperatures were estimated with the garnet–clinopyroxene thermometer of Powell (1985) and, due to the absence of paragonite, minimum pressures are constrained by the breakdown of paragonite to kyanite + omphacite(Jd_{50}) + vapour (Holland 1979). Peak pressures were estimated with phengite barometry based on the equilibrium assemblage garnet + omphacite + phengite (Waters and Martin 1993) and the corresponding temperatures were calculated using the Powell (1985) garnet–clinopyroxene and the Green and Hellman (1982) garnet–phengite thermometer, following the procedure of Carswell et al. (1997). Temperature estimates were obtained from eight localities distributed throughout the eclogite zone (Fig. 2; Table 7). Although disequilibrium textures are common features of these eclogites, only eclogites that were "well equilibrated" or that contain equilibrated subdomains were used for P–T

Table 6 Representative phengite analyses and structural formulae. Structural formulae on the basis of 11 oxygens

Sample	Z 101–5	Z 101–7	Z 101–11
Analysis	phe1p17	phe1p2	phe1p3
Location	Rim	Rim	Rim
SiO_2	51.31	51.00	47.93
TiO_2	0.32	0.30	0.54
Al_2O_3	25.80	26.08	29.06
Cr_2O_3	0.06	0.07	0.02
FeO	1.54	1.24	1.87
Fe_2O_3	–	–	–
MgO	4.28	4.19	3.19
MnO	0.01	0.00	0.01
CaO	0.00	0.04	0.01
Na_2O	0.21	0.19	0.70
K_2O	11.04	11.14	10.37
Total	94.56	94.25	93.71
Si	3.448	3.436	3.260
Al^{IV}	0.552	0.564	0.740
Al	1.491	1.507	1.590
Ti	0.016	0.015	0.028
Cr	0.003	0.004	0.001
Fe^{2+}	0.087	0.070	0.106
Fe^{3+}	0.000	0.000	0.000
Mg	0.429	0.421	0.323
Mn	0.000	0.000	0.001
Ca	0.000	0.003	0.001
Na	0.027	0.025	0.092
K	0.946	0.958	0.900
Total	7.000	7.002	7.042
XFe	0.17	0.14	0.25
Cl wt%	0.20	0.14	0.10

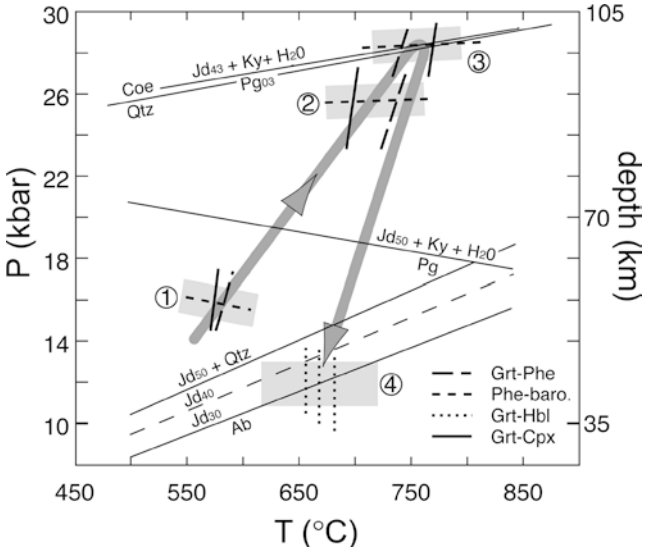

Fig. 8 P–T diagram for the phengite-bearing eclogites with reaction curves limiting peak metamorphic conditions and P–T path derived from petrographic observations and thermobarometric results. *Shaded boxes* indicate pressure and temperature uncertainties for prograde, peak and retrograde metamorphic stages. (*1*) Z 101–11a: Grt_{core}–Omp_{core}–Phe_{incl}; (*2*) Z 101–5: Grt_{rim}–Omp_{rim}–Phe_{matrix}; (*3*) Z 101–7: Grt_{rim}–Omp_{rim}–Phe_{matrix}; (*4*) Z 101–5,7,11a: Grt–Amp. Coesite = quartz after Mirwald and Massonne (1980)

estimates. The attainment of equilibrium during eclogite facies metamorphism within subdomains was tested by comparing P–T results from five to ten mineral pairs. Assuming $Fe^{2+} = Fe^{tot}$, garnet and omphacite rim compositions give peak-metamorphic temperatures between 710 and 760 °C for seven localities, and ca. 885 °C for the eighth locality (Z 101), at a minimum pressure of 20 kbar as suggested by the coexistence of Jd_{50} with kyanite (Table 7). Temperatures are ca. 100 °C lower if the calculated Fe^{3+}-contents in omphacite and garnet are considered, yielding values between 605 and 665 °C, and 715 °C (Z 101). Due to uncertainties in calculating Fe^{3+}-contents from microprobe analyses, the spread of calculated temperatures for each locality is greater than for the case when Fe^{2+} as Fe^{tot} is assumed (Table 7). Temperatures calculated assuming $Fe^{2+} = Fe^{tot}$ give maximum values whereas the temperature calculations considering Fe^{3+}-contents give lower values. This is because Fe^{3+}/Fe^{tot} ratios can reach ca. 0.60 in omphacite but only ca. 0.05 in garnet (Tables 3, 4). The calculated Fe^{3+}/Fe^{tot} ratios are in agreement with values obtained from other eclogite occurrences, where omphacite usually has almost ten times higher Fe^{3+}/Fe^{tot} ratios than coexisting garnet (Carswell et al. 1997, 2000). Thus, the temperatures from the calculations considering Fe^{3+}-contents are interpreted to be more realistic than the ones assuming $Fe^{2+} = Fe^{tot}$. Excluding the higher temperatures from locality Z 101, all eclogites equilibrated between 605 and 665 °C at minimum pressures of 20 kbar. This temperature range of ca. 60 °C is remarkably small, considering the great spatial distribution of the eclogite occurrences regarded here (Fig. 2). Peak pressure estimates for the eclogite occurrences, obtained from phengite-bearing eclogites (locality Z 101), are about 26–28 kbar (Fig. 8; Table 8). P–T conditions of a prograde metamorphic stage of the clockwise P–T path were deduced from phengite inclusions in garnet. Garnet and omphacite cores, together with phengite inclusions, give 580 ±30 °C at 15.8 ±2.5 kbar, while peak-metamorphic conditions estimated from garnet and omphacite rims and matrix phengites are 720 ±40 °C at 25.6 ±2.5 kbar for sample Z 101–5 and 755 ±40 °C at 28.3 ±2.5 kbar for sample Z 101–7 (Fig. 8). Applying the internally consistent data set of Berman (1988), these high pressures are supported by the low paragonite content (ca. 3 mol%) of white

Table 7 Temperature estimates (in °C) for minimum pressures of 20 kbar for eclogites from eight localities. Fe^{2+} as Fe^{tot}, Fe^{3+} calculated by stoichiometric charge balance

[a]Minimum error 25°

Location	Z 101	Z 135	Z 139	Z 143	Z 146	Z 216	Z 249	Z 310
Mean Fe^{2+}	885	725	755	725	730	715	760	730
Error[a]	±25	±25	±40	±25	±25	±25	±25	±42
Mean Fe^{3+}	715	630	605	635	630	625	640	665
Error[a]	±32	±25	±28	±50	±40	±48	±25	±40

Table 8 Pressure and temperature estimates from the phengite-bearing eclogites

Sample	Grt–Hbl Thermometry (°C)	Grt–Cpx[a]	Grt–Phe	Phe Barometry (kbar)	Pg#	Remarks
	±50	±25	±25	±2.5		
Z 101–5	670	700	735	25.6	–	Grt–Hbl only $Fe^{2+} = Fe^{tot}$. Peak-pressures
Z 101–7	680	770	740	28.3	–	are 1.5 kbar (Z 101–5) and 0.5 kbar (Z 101–7) lower applying the barometer version 1996 www.earth.ox.ac.uk/~davewa/research/ecbarcal.html
Z 101–11	655	575	580	15.8	–	All calculations with $Fe^{2+} = Fe^{tot}$

[a]For peak condition estimates of phengite-bearing eclogites less grt–cpx pairs were used than for temperature estimates only (Table7)

mica in equilibrium with omphacite and kyanite (Z 101–7; Fig. 8). Pressures of about 26–28 kbar at the temperature range of consideration (630–760 °C, including all estimates) indicate that these rocks may almost have reached the stability field of coesite and thus ultra-high pressure metamorphism. The temperatures at the calculated peak pressures are only slightly higher than those at minimum pressures (605–715 °C, without locality Z 101). Even if the upper limit of the uncertainties of the pressure calculations is considered (± 2.5 kbar, Waters and Martin 1993) all but one lie below the coesite stability field (Fig. 8). It is reasonable that ultra-high pressure conditions have not been attained since no mineralogical evidence beside the phengite barometry was found, such as coesite relics, palisade-quartz inclusions in garnet, K-rich clinopyroxenes, or Na-bearing garnet.

Since evidence for a direct transformation from gabbro to eclogite (Figs. 5, 7a, b) was found in many samples, we infer that metamorphism and thus eclogitisation took place probably at temperatures between 630 and 690 °C and pressures of about 26–28 kbar. Hence, it implies an overstepping of the eclogitisation reactions by at least 10 kbar, if the albite breakdown to jadeite and quartz is used as the final boundary to an eclogite (Austrheim 1998). This approach results in a minimum value for the degree of overstepping since the gabbroic plagioclase is usually more calcic and thus starts to react under lower P–T conditions (Wayte et al. 1989). The estimated degree of overstepping is in accordance with other estimates given for crustal rocks that experienced a kinetically delayed eclogitisation during continental collision (Austrheim 1998).

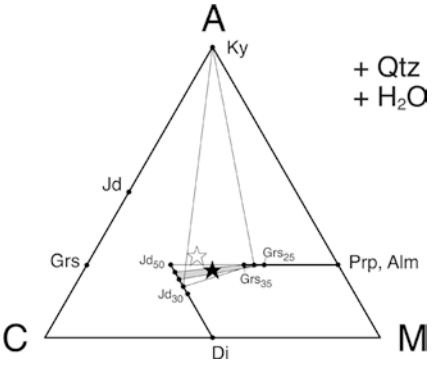

Fig. 9 ACM diagram (after Thompson 1981) illustrating the phase relations of the Zambian mafic rocks during their metamorphic evolution. Condensed CMASH composition space, with projection from Qtz and H_2O and condensation along $NaSiCa_{-1}Al_{-1}$ (for more details see Thompson 1981). The mean composition of the rocks is indicated by the *black star*; the *white star* indicates the possible composition of Al-rich subdomains. The *shaded triangle* represents the peak metamorphic assemblages of the "completely" equilibrated eclogites, while the three-phase field Omp–Grs–Ky represents the peak assemblage of eclogites that contain relics of magmatic pyroxene (i.e. Z 216–5 and Z 310–4)

The protoliths of the Zambian eclogites had MORB-like (mid-ocean ridge basalt) major and trace element compositions (John et al. 2003a) and the formation of Ky-bearing eclogites from such protoliths is unusual, since average MOR-basalts are Al-poor rocks and no kyanite should be formed. This is illustrated in Fig. 9 in which the Zambian eclogites (black star) plot into a two-phase field (Grt–Cpx) of the projection and thus do not contain enough Al to form kyanite in addition to garnet and omphacite under peak metamorphic conditions. A more aluminous composition is required. For certain subdomains within the Ky-bearing eclogites, the necessary shift to Al-rich composition (white star in Fig. 9) resulted from "extraction" of the Al-poor parts from the transforming rock, i.e. relics of magmatic clinopyroxene (e.g. Fig. 7b). In contrast, Al-rich parts of the rock, i.e. former plagioclase, reacted completely to kyanite-bearing assemblages (e.g. Fig. 7a). Another possible scenario for such a shift is that kyanite precipitated from an Al-supersaturated fluid in a vein (e.g. Fig. 4b). Thus, the occurrence of kyanite in eclogite facies rocks with MORB-like compositions is only possible in (1) incompletely equilibrated rocks that contain magmatic pyroxene relics (extraction of Al-poor parts from the bulk-chemical system), or in (2) Al-rich chemical subdomains (e.g. former plagioclase sites or veins – precipitated from Al-supersaturated fluids).

Processes during eclogitisation

The porphyroblastic eclogites (group 2) contain no textural evidence for specific kinematic conditions which may have occurred during the transformation from gabbro to eclogite. In contrast, the preserved gabbroic

textures in the group 1 eclogites clearly indicate that for these rocks eclogitisation occurred without ductile deformation (Fig. 3a) and omphacite inclusions in garnet (Fig. 5, Fig. 7b) are evidence that metamorphism commenced under eclogite facies conditions. In addition, the sheared porphyroclastic textures of group 3 eclogites are the result of ductile deformation. The mineral assemblages formed within pressure shadows (Fig. 7a) in these rocks suggest that the transformation took place under eclogite facies conditions. Hence, the different textures of the Zambian eclogites indicate that kinematic conditions that existed during eclogitisation varied locally. However, all reactions in the different types of eclogites, which are related to the gabbro-to-eclogite transformation, are based on net transfer reactions. There was always more than one reactant necessary to produce the eclogite facies peak assemblages. Therefore, once the transformation started, sustained material transport was essential for the continued production of eclogite facies assemblages during metamorphism. Some processes of material transport and features of the gabbro-to-eclogite transformation are discussed below.

Dissolution and precipitation mechanism to form metamorphic minerals

Element exchange between minerals, resulting from changing P, T and X, occurs by diffusion or net transfer reactions. Diffusion in a rock occurs in response to chemical potential gradients and results in element exchange within a mineral or between minerals over grain boundaries and has no effect on the physical characteristics of the related minerals such as the size, form and modal abundance. In contrast, net transfer reactions between minerals are based on dissolution of mineral phases and growth of one or more mineral phases (e.g. Carmichael 1969; Ridley and Thompson 1985; Spear 1993). The preservation of undeformed, gabbroic textures in group 1 eclogites must be the consequence of pure fluid–rock interaction. Plagioclase breakdown [Pl $\Rightarrow$ Grs + Jd + Ky + Qtz, reaction (4)], the breakdown of augitic pyroxene, and the related growth of omphacite [e.g. $CaMg_{(\text{in augite})} \Leftrightarrow NaAl_{(\text{in fluid})}$] are all based on net transfer reactions and are thus dependent on dissolution, transport and precipitation processes. In the first case, the consumption of plagioclase and the production of quartz, jadeite, grossular and kyanite clearly affects the modal proportions of the involved minerals. During the replacement of magmatic augite by omphacite (Fig. 10), grain boundaries move as a consequence of coupled augite consumption and omphacite growth, which indicates that the minerals were replaced by dissolution of the educt and precipitation of the product phases and significant diffusion operated only within the acting fluid. The importance of the dissolution and precipitation mechanisms for the gabbro-to-eclogite transformation is also demonstrated by the sheared

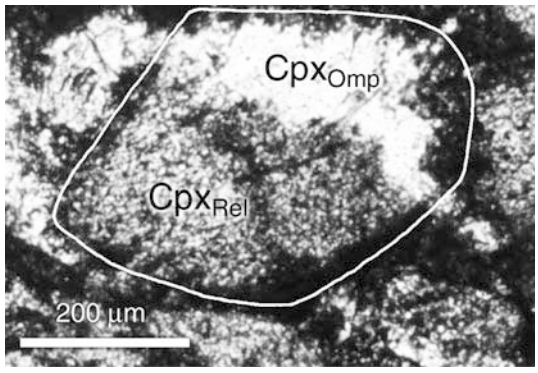

Fig. 10 Omphacite (Cpx_{Omp}, Jd_{35}) in sample Z 310–4 replacing former magmatic pyroxene (Cpx_{Rel}, Jd_{10}) . Note that the grain boundary between Cpx_{Rel} and Cpx_{Omp} has moved during replacement by consumption of Cpx_{Rel} and growth of Cpx_{Omp}

eclogites (group 3). The chemical profile across the pyroxene porphyroclasts shown in Fig. 7a shows a characteristic asymmetry. A gentle compositional gradient from Cpx_{Omp} to Cpx_{Rel} is observed on one side of the grain while on the other side the transition is marked by a sharp compositional change (Fig. 7a). This asymmetry may be explained by fluid flow acting during the pressure solution. Hence, the formation of the flat gradient at the reaction front is related to the continuous dissolution of the magmatic pyroxene (Cpx_{Rel}), and the simultaneous precipitation of omphacite (Cpx_{Omp}), which grew topotactically on Cpx_{Rel} at the site of dissolution. This may occur when a fluid, saturated with Al and Na (from dissolved Pl), arrives at the reaction front of a magmatic relic. After dissolving some of the Cpx_{Rel}, the fluid becomes supersaturated with respect to Cpx_{Omp} components for the P–T conditions of the given subdomain, causing precipitation of Cpx_{Omp} at the solution front. Continued dissolution of Cpx_{Rel} and precipitation of Cpx_{Omp} decreases the concentrations of Al and Na within this particular subdomain, whereas the concentrations of Ca, Mg and Fe increase in the fluid. This results in a decrease of the Jd-content towards the core of the magmatic relic and creates the smooth transition between the rim and unaffected core in areas undergoing pressure solution. If the whole pyroxene (including solution front, magmatic relic and pressure shadow) is considered as a subsystem, omphacite, quartz and kyanite precipitated from the fluid within the pressure shadow (Fig. 7a), because the fluid was supersaturated with respect to these minerals. The sharp compositional transition between the core of the magmatic relic and the omphacite grown in the pressure shadow indicates that significant diffusion occurred only within the fluid and not across grain boundaries.

As discussed above, all mineral reactions that transformed the gabbros into eclogites operated via dissolution of the reactant(s), material transport and precipitation of the product(s). Material transport necessary for mineral reactions occurred only through a fluid (Carmichael 1969; Walther and Wood 1984).

Usually, the growth of metamorphic mineral assemblages is interpreted to be controlled by deformation combined with fluid availability (e.g. Koons et al. 1987). However, since magmatic relics are very common in the sheared as well as in the "gabbro-textured" eclogites of Zambia, the degree of eclogitisation was apparently limited by the rates of the dissolution–transport–precipitation processes and thus related to the fluid/rock ratio, rather than the degree of ductile deformation.

Formation of pseudomorphs

Three types of pseudomorphic replacements are responsible for the preservation of gabbroic textures within the eclogites. Two of them developed during prograde metamorphism, and the third may have developed during retrogression. The first type is the polymineralic replacement of plagioclase by garnet, omphacite, kyanite and quartz (Figs. 3c, 5, 7b), and the second type comprises monomineralic replacements, e.g. of augite by omphacite and of plagioclase by garnet (Fig. 3a). The third type is the transformation of the magmatic pyroxene relics to low-Jd pyroxenes and amphiboles (Figs. 3c, 7b).

Pseudomorphs are created by the dissolution of the reactant accompanied by the simultaneous precipitation of the product phase(s), which inherits the shape of the reactant crystal (Carmichael 1969; Merino and Dewers 1998). Pseudomorphs can be formed during the prograde evolution when the molar volumes of the replacement products are lower than the molar volume of the reactant and the "force of crystallisation" is supporting the mineral growth at the site of dissolution (Ferry 2000). They can also be formed during the retrograde evolution depending on the difference between the molar volumes of reactants and products (Ferry 2000), or may be independent of it but related to the flux of material (e.g. Merino and Dewers 1998).

In the eclogites studied here, the pseudomorphic replacement of plagioclase by a fine grained eclogite facies intergrowth (Grt–Omp–Ky–Qtz) is attributed to the first type of replacements. The very fine grain size (ca. 10 μm) of the reaction products is consistent with the model in which rapid nucleation of the product phases is triggered by fluid influx in a metastable system (Rubie 1983, 1998) and thus requires that plagioclase persisted as a metastable phase well outside of its stability field. In this case, the mineral reaction apparently needed to be triggered by a fluid which dissolved the plagioclase as well as some of the metastable augitic pyroxene. The dissolution of the Pl and Aug was accompanied by precipitation of the fine grained Grt–Omp–Ky–Qtz intergrowth at the site of the former plagioclase. Metastable plagioclase is rare but has been found in low-T/high-P environments (e.g. Austrheim 1986/87; Wayte et al. 1989). Rubie (1998) described cases in which plagioclase in a dry system was metastable at pressures >7 kbar above the equilibrium boundary [reaction (4)].

The monomineralic replacements, such as garnet pseudomorphs after plagioclase (type two), run in two steps. The first step is dissolution of the host mineral and simultaneous nucleation of the new mineral directly at the site of dissolution, which may occur along grain boundaries and cracks (e.g. Mørk 1985a, 1985b). After this initial process, effective material exchange between the dissolving plagioclase and magmatic pyroxene ($Na + Al \Leftrightarrow Fe + Mg + Ca$) during the growth of omphacite and garnet is necessary to form the inclusion-poor pseudomorphs that are chemically different from the replaced minerals. Thus, the amount of fluid had to be reasonably high in these domains (e.g. Mørk 1985a, 1985b).

The retrograde pseudomorphic replacements (third type) are characterised by the replacement of the magmatic pyroxene, which survived the peak eclogite facies metamorphism, by low-jadeite pyroxene and amphibole. The new pyroxene, which has a lower molar volume, replaces the magmatic relic, while the higher molar volume amphibole grew within the former cleavage planes of the magmatic pyroxene. Together, both fill the available space. The omphacitic replacement products often inherited the twinning from the magmatic relics (Fig. 3c). In this case simultaneous, topotactic growth of the secondary mineral at the site of dissolution is required (Turner and Weiss 1965; Carmichael 1987), which in turn demands a restricted amount of reacting material per time so that the product can react with the host crystal during the topotactic growth (e.g. Kleber 1962).

The transport of material and therefore the amount and the mobility of the transport medium is important in controlling the textures (Carmichael 1969). A strongly supersaturated transport medium (fluid) will result in rapid precipitation and short-distance transport of material (Ferry 2000), especially if a large overstepping of the equilibrium conditions occurred before the fluid infiltrated the system. If a large amount of fluid is available, however, material transport is enhanced. This is because at lower concentrations of dissolved components in the fluid, fast precipitation is not forced and transport over longer distances is possible (Walther and Wood 1984). Hence, the occurrence of prograde and retrograde pseudomorphic replacements is mainly controlled by the fluid/rock ratio, which in turn controls the material flux within the particular subdomains.

Vein formation

The veins of the eclogites are interpreted to be part of a late-stage, prograde fluid infiltration, which is indicated by similar chemical compositions of vein and host minerals and by similar results obtained from P–T calculations of veins and hosts, as well as their textural relations. In some cases, the veins provided pathways for

fluid influx into the system. Veins that were formed during prograde metamorphism and at peak eclogite facies conditions are a common feature elsewhere (e.g. Austrheim 1986/87, 1990; Engvik et al. 2001; Gao and Klemd 2001). The volume reduction of the host rock during prograde metamorphism (gabbro-to-eclogite) may have provided the necessary space, since mineral reactions could enhance the permeability (Rumble et al. 1982; Aharonov et al. 1997). This might have resulted in channelised fluid flow along fractures which then evolved to veins as visible in Fig. 3b. Hydrofracturing could increase the available pore volume, which would decrease fluid pressure and cause the vein minerals to precipitate (Brunsmann et al. 2000; Gao and Klemd 2001). Other veins, however, might be related to fluid-channeling caused by shearing. In most cases, the constituent elements of vein-forming minerals were most likely extracted from the immediate surroundings, at or near the time of peak metamorphic temperature. Vein opening and the crystallisation of vein minerals are supposed to occur simultaneously (Vidale 1974; Ferry 2000; Widmer and Thompson 2001). Since kyanite is a common vein-forming mineral (Fig. 4b) in the Al-poor Zambian eclogites, a high mobility of alumina in the eclogitic fluid is required, which seems to be not an unusual feature under eclogite facies conditions, as shown by Widmer and Thompson (2001). The vein shown in Fig. 3b (Z 301–4), containing omphacite, epidote-group minerals and garnet, is mineralogically similar to the MORB-type epidote–eclogites (Grt–Omp–Ep) experimentally produced by Schmidt and Poli (1998). P–T estimates obtained for this vein's host rock are in agreement with the experimentally determined stability field (20–30 kbar and 660–800 °C) and the high epidote/garnet ratio of the vein assemblage indicate a water-saturated system [reaction (5) vs. (4); Schmidt and Poli 1998]. Since the host contains a lot of magmatic relics (Figs. 3b and 7b), this vein may represent a fluid infiltration pathway into a metastable gabbro from which eclogitisation affected the rock due to accompanied fluid influx along grain boundaries.

Fluid source

Due to the lack of fluid inclusions in the Zambian eclogites, the ability of OH-bearing minerals to incorporate chlorine was used to estimate roughly the fluid composition during the metamorphic evolution. Kullerud (1996) proposed that the Cl-content of amphibole and biotite is principally controlled by the activity ratio $a_{Cl}-/a_{OH}-$ in the fluid in equilibrium with the growing minerals. Since silicates preferentially incorporate OH over Cl, a high $a_{Cl}-/a_{OH}-$ ratio is required to form Cl-bearing silicates (e.g. Kullerud 1996). A chlorine-rich fluid can be produced by the desiccation mechanism (e.g. Markl and Bucher 1998), in which a fluid becomes enriched in chlorine due to continuous hydration reactions in a fluid-poor system. However, the Cl-contents of amphiboles and phengites of the Zambian eclogites were high throughout the entire metamorphic evolution (e.g. up to 5.8 wt% for peak amphiboles and 0.2 wt% for peak phengites; Tables 5, 6). Evidence for prograde metamorphic reactions prior to eclogite facies conditions was not found. Instead all eclogites formed directly from gabbroic protoliths. Fluid influx into the gabbroic protoliths can originate either from external rock sources during subduction (e.g. Wayte et al. 1989) or from seawater-alteration of the oceanic crust before subduction (e.g. Pognante 1985; Barnicoat and Cartwright 1997). Since there is no petrographic evidence for seawater alteration in unmetamorphosed gabbros, and no prograde blueschist or amphibolite facies relics were found, the protoliths of the eclogites were probably too dry to contain the source of the eclogitic fluid. Hence, significant interaction with early hydrothermal fluids at the mid-ocean ridge can most likely be ruled out for the investigated rocks. Considering the relatively deep position of gabbros in a typical oceanic crust, fluids released by the blueschist-to-eclogite transformation of the upper oceanic crust are unlikely, since blueschists start to dehydrate at lower depths and the fluids will tend to migrate upward (Peacock 1990). A more likely source for the fluid is the serpentinised part of the underlying slab (Scambelluri et al. 1997; Schmidt and Poli 1998). Scambelluri et al. (1997) deduced from fluid inclusions and mineral chemical data that an eclogite facies fluid was derived from a seawater-altered peridotite and formed syn-eclogitic veins at about 25 kbar and 550–600 °C. This fluid was rich in Cl, Na, K, Mg and Fe. The high chlorine content of the fluid is interpreted as being the result of hydration of mantle minerals and the formation of hydrous vein minerals (desiccation) during prograde metamorphism (Scambelluri et al. 1997). Such a fluid can act as a catalyst for the metamorphic reactions within the eclogites and may have delivered the material necessary for the formation of the potassium-rich Cl-amphiboles that occur in eclogite facies veins (e.g. Fig. 4), as well as the peak metamorphic Cl-bearing phengites in the Zambian eclogites. The fluid that entered these rocks may derive from serpentine and chlorite breakdown in seawater-altered mantle (Schmidt and Poli 1998) below the gabbroic protoliths of the Zambian eclogites.

Discussion and conclusions

The dissolution and precipitation features in the Precambrian eclogites described in this study imply that a free fluid phase must have been present during the gabbro-to-eclogite transformation. This conclusion is supported by the occurrence of prograde eclogitic veins which also require a free fluid phase. The fluid had a high chlorinity as indicated by Cl-rich amphiboles and phengites formed during different stages of the metamorphic evolution. Omphacites and most of the epidotes in some eclogitic veins (Fig. 3b) consist of tiny

subgrains and some eclogite facies mineral intergrowths that have replaced plagioclase are also fine grained (Figs. 5, 7b). These small grain sizes are interpreted to reflect very fast nucleation caused by fluid influx into a dry rock that contained a metastable mineral assemblage due to overstepping. Thus, fluid infiltration and the fluid/rock ratio are apparently limiting factors during the gabbro-to-eclogite transformation which occurred in the studied case after equilibrium phase boundaries had been crossed and the rocks were under eclogite facies P–T conditions. Even in rocks that were ductile deformed, the fluid/rock ratio controlled the reaction and limited reaction rates due to material transport. Fluid availability is thus the key factor for governing the gabbro-to-eclogite transformation. Considering the close spatial association of gabbros and eclogites in the Zambezi Belt and assuming that a hydrated mantle underlying these rocks was the fluid source, it seems that the liberated fluid infiltrated along channels the gabbroic part of the oceanic crust. Since part of the gabbros transformed directly to eclogites and P–T estimates record ca. 630 to 690 °C at pressures above 20 kbar (and probably at 26–28 kbar), it is most likely that the dehydration of the subcrustal part of the slab started only after a critical depth had been reached. This interpretation is in agreement with the recent models for slab dehydration (e.g. Schmidt and Poli 1998; Rüpke et al. 2002). The textural preservation of disequilibrium caused by incomplete reactions indicates that the processes that transformed the gabbros to eclogites affected some of the investigated eclogites for only a limited time. This suggests that either (1) the eclogites did not remain long enough at great depth for reactions to run to completion or (2) the fluids, which catalysed the reactions, left the rock systems. Since fully equilibrated eclogites as well as eclogites with magmatic relics are found, the residence time at great depth is unlikely to be the limiting factor. This indicates that under boundary conditions, like those experienced by the Zambian rocks, mineral reactions only occur in the presence of a fluid phase. Moreover, the preservation of relic magmatic minerals, as well as gabbroic textures, and the evidence for channelised fluid flow triggering eclogitisation, makes it reasonable that the untransformed gabbros and the eclogites of the investigated zone in the Zambezi Belt are co-genetic. However, they experienced different fluid and consequently metamorphic transformation histories. Many of the Zambian eclogites contain kyanite although they have Al-poor MORB-like bulk-compositions. Most likely, this is due to the preservation of small-scale, chemically different subdomains (former mineral grains, veins) that are not in equilibrium. The preservation of prograde disequilibrium features makes a polymetamorphic history for the investigated rocks most unlikely.

Acknowledgements The Deutsche Forschungsgemeinschaft (DFG) funded this research through grants Sche 265–10/1, 10/2 and 265/S1–1. We thank A. Kronz and P. Appel for advice during microprobe work. Further thanks are due to K. Pollok and F. Tembo for fruitful discussions which greatly improved this study. We thank the University of Zambia and the Geological Survey of Zambia for support during fieldwork. The constructive reviews of H. Austrheim and an anonymous reviewer led to a considerable improvement of the manuscript. This publication is contribution no. 29 of the Sonderforschungsbereich 574 "Volatiles and Fluids in Subduction Zones" at Kiel University.

References

Aharonov E, Spiegelmann M, Kelemen P (1997) Three-dimensional flow and reaction in porous media: implications for the Earth's mantle and sedimentary basins. J Geophys Res 102:14821–14833

Austrheim H (1986/87) Eclogitisation of lower crustal granulites by fluid migration through shear zones. Earth Planet Sci Lett 81:221–232

Austrheim H (1990) The granulite–eclogite facies transition: a comparison of experimental work and a natural occurrence in the Bergen Arcs, western Norway. Lithos 25:163–169

Austrheim H (1998) Influence of fluid and deformation on metamorphism of the deep crust and consequences for the geodynamics of collision zones. In: Hacker BR, Liou JG (eds) When continents collide: geodynamics and geochemistry of ultrahigh-pressure rocks. Kluwer Academic, Dordrecht, pp 297–323

Barnicoat AC, Cartwright I (1997) The gabbro–eclogite transformation: an oxygen isotope and petrographic study of west Alpine ophiolites. J Metamorph Geol 15:93–104

Berman RG (1988) Internally-consistent thermodynamic data for minerals in the system Na_2O–K_2O–CaO–MgO–FeO–Fe_2O_3–Al_2O_3–SiO_2–TiO_2–H_2O–CO_2. J Petrol 29:445–522

Brunsmann A, Franz G, Erzinger J, Landwehr D (2000) Zoisite- and clinozoisite segregations in metabasites (Tauern window, Austria) as evidence for high-pressure fluid–rock interaction. J Metamorph Geol 18:1–21

Cahen L, Snelling NJ, Delhal J, Vail JR (1984) The geochronology and evolution of Africa. Clarendon, Oxford

Carmichael DM (1969) On the mechanism of prograde metamorphic reactions in quartz-bearing pelitic rocks. Contrib Mineral Petrol 20:244–267

Carmichael DM (1987) Induced stress and secondary mass transfer: thermodynamic basis for tendency toward constant-volume constraint in diffusion metasomatism. In: Helgeson HC (ed) Chemical transport in metasomatic processes. Reidel, Dordrecht, pp 239–264

Carswell DA, O'Brien PJ, Wilson RN, Zhai M (1997) Thermobarometry of phengite-bearing eclogites in the Dabie Mountains of central China. J Metamorph Geol 15:239–252

Carswell DA, Wilson, RN, Zhai M (2000) Metamorphic evolution, mineral chemistry and thermobarometry of schists and orthogneisses hosting ultra-high pressure eclogites in the Dabieshan of central China. Lithos 52:121–155

Engvik AK, Austrheim H, Erambert M (2001) Interaction between fluid flow, fracturing and mineral growth during eclogitization, an example from the Sunnfjord area, Western Gneiss Region, Norway. Lithos 57:111–141

Ferry JM (2000) Patterns of mineral occurrence in metamorphic rocks. Am Mineral 85:1573–1588

Gao J, Klemd R (2001) Primary fluids entrapped at blueschist to eclogite transition: evidence from the Tianshan meta-subduction complex in northwestern China. Contrib Mineral Petrol 142:1–14

Goscombe B, Armstrong R, Barton JM (1998) Tectonometamorphic evolution of the Chewore inliers: partial re-equilibration of high-grade basement during the Pan-African Orogeny: J Petrol 39.1347–1384

Goscombe B, Armstrong R, Barton JM (2000) Geology of the Chewore Inliers, Zimbabwe: constraining the Mesoproterozoic

to Palaeozoic evolution of the Zambezi Belt. J Afr Earth Sci 30:589–627
Green D, Hellman PL (1982) Fe–Mg partitioning between coexisting garnet and phengite at high pressures, and comments on a garnet–phengite geothermometer. Lithos 15:253–266
Hacker BR (1996) Eclogite formation and the rheology, buoyancy, seismicity, and H_2O content of oceanic crust. In: Bebout GE, Scholl DW, Kirby SH, Platt JP (eds) Subduction top to bottom. Geophysical Monograph vol 96, pp 337–346
Hanson RE, Wilson TJ, Brueckner HK, Onstott TC, Wardlaw M, Johns CC, Hardcastle KC (1988) Reconnaissance geochronology, tectonothermal evolution, and regional significance of the middle Proterozoic Choma–Kalomo Block, southern Zambia. Precambrian Res 42:39–61
Hanson RE, Wilson TJ, Munyanyiwa H (1994) Geologic evolution of the Neoproterozoic Zambezi Orogenic Belt in Zambia. J Afr Earth Sci 18:135–150
Holland TJB (1979) Experimental determination of the reaction Paragonite = Jadeite + Kyanite + H_2O, and the consistent thermodynamic data for part of the system Na_2O–Al_2O_3–SiO_2–H_2O, with applications to eclogites and blueschists. Contrib Mineral Petrol 68:292–301
John T, Schenk V, Haase K, Scherer EE, Tembo, F (2003a) Evidence for a Neoproterozoic ocean in south central Africa from MORB-type geochemical signatures and P–T estimates of Zambian eclogites. Geology 31:243–246
John T, Schenk V, Mezger K, Tembo F (2003b) Timing and P–T evolution of whiteschist metamorphism in the Lufilian Arc–Zambezi Belt orogen (Zambia): implications to the Gondwana assembly. J Geol (in press)
Johnson SP, Oliver GJH (2002) High *f*O2 metasomatism during whiteschist metamorphism, Zambezi Belt, Northern Zimbabwe. J Petrol 43:271–290
Kirby SH, Engdahl ER, Denlinger R (1996) Intermediate-depth intraslab earthquakes and arc volcanism as physical expressions of crustal and uppermost mantle metamorphism in subducting slabs. In: Bebout GE, Scholl DW, Kirby SH, Platt JP (eds) Subduction top to bottom. Geophysical Monograph vol 96, pp 195–214
Kleber W (1962) Über orientierte heterogene Keimbildung in kristallisierten Phasen. Forsch Fortschr 36:257–262
Koons PO, Rubie DC, Frueh-Green G (1987) The effects of disequilibrium and deformation on the mineralogical evolution of quartz diorite during metamorphism in the eclogite facies. J Petrol 28:679–700
Kretz R (1983) Symbols for rock-forming minerals. Am Mineral 68:277–279
Kullerud K (1996) Chlorine-rich amphiboles: interplay between amphibole composition and an evolving fluid. Eur J Mineral 8:355–370
Leake BE, Wooley AR, Arps CES, et al. (1997) Nomenclature of amphiboles; report of the Subcommittee on Amphiboles of the International Mineralogical Association Commission on New Minerals and Mineral Names. Eur J Mineral 9:623–651
Markl G, Bucher K (1998) Compositions of fluids in the lower crust inferred from metamorphic salt in lower crustal rocks. Nature 391:781–783
Merino E, Dewers T (1998) Implications of replacement for reaction-transport modelling. J Hydrol 209:137–146
Mirwald PW, Massonne H-J (1980) The low–high quartz and quartz–coesite transition to 40 kbar between 600° and 1600 °C and some reconnaissance data on the effect of $NaAlO_2$ component on the low quartz–coesite transition. J Geophys Res 85:6983–6990
Morimoto N, Fabries J, Ferguson AK, Ginzburg IV, Ross M, Seifert FA, Zussman J, Aoki K, Gottardi G (1988) Nomenclature of pyroxenes. Am Mineral 73:1123–1133
Mørk MBE (1985a) A gabbro to eclogite transition on Flemsøy, Sunnmøre, western Norway: Chem Geol 50:283–310
Mørk MBE (1985b) Incomplete high P–T metamorphic transitions within the Kvamsøy pyroxenite complex west Norway: a case study of disequilibrium. J Metamorph Geol 3:245–264
Peacock SM (1990) Fluid processes in subduction zones. Science 248:329–337
Pognante U (1985) Coronitic reactions and ductile shear zones in eclogitised ophiolite metagabbros, Western Alps, North Italy. Chem Geol 50:99–110
Porada H, Berhorst V (2000) Towards a new understanding of the Neoproterozoic–Early Palaeozoic Lufilian and northern Zambezi Belts in Zambia and the Democratic Republic of Congo. J Afr Earth Sci 30:727–771
Powell R (1985) Regression diagnostics and robust regression in geothermometer/geobarometer calibration: the garnet–clinopyroxene geothermometer revisited. J Metamorph Geol 3:231–243
Ridley J, Thompson AB (1985) The role of mineral kinetics in the development of metamorphic microtextures. In: Walther JV, Wood BJ (eds) Fluid–rock interaction during metamorphism. Springer, Berlin Heidelberg New York, pp 154–193
Rubie DC (1983) Reaction-enhanced ductility: the role of solid–solid univariant reactions in deformation of the crust and mantle. Tectonophysics 96:331–352
Rubie DC (1998) Disequilibrium during metamorphism: the role of nucleation kinetics. In: Treloar PJ, O'Brien P (eds) What drives metamorphism and metamorphic reactions? Geological Society, London, Special Publications vol 138, pp 199–214
Rüpke LH, Phipps Morgan J, Hort M, Connolly JAD (2002) Are the regional variations in Central America arc lavas due to differing basaltic versus peridotitic slab sources of fluid? Geology 30:1035–1038
Rumble D III, Ferry JM, Hoering TC, Boucot AJ (1982) Fluid flow during metamorphism at the Beaver Brook fossil locality. Am J Sci 282:866–919
Scambelluri M, Piccardo GB, Philippot P, Robbiano A, Negretti L (1997) High salinity fluid inclusions formed from recycled seawater in deeply subducted alpine serpentinite. Earth Planet Sci Lett 148:485–499
Schenk V, Appel P (2001) Anti-clockwise P–T path during ultrahigh-temperature (UHT) metamorphism at ca. 1050 Ma in the Irumide Belt of Eastern Zambia. Berichte der Deutschen Mineralogischen Gesellschaft. Beih Eur J Mineral 13:161
Schmidt MW, Poli S (1998) Experimentally based water budgets for dehydrating slabs and consequences for arc magma generation. Earth Planet Sci Lett 163:361–379
Sikatali C, Legg CA, Bwalya JJ, Ng'ambi O (1994) Geological and mineral occurrence map (1:2,000,000). Geological Survey of Zambia
Spear FS (1993) Metamorphic phase equilibria and pressure–temperature–time paths. Monograph series, Mineralogical Society of America
Tembo F, Kampunzu AB, Porada H (1999) Tholeiitic magmatism associated with continental rifting in the Lufilian Fold Belt of Zambia. J Afr Earth Sci 28:403–425
Thieme JG (1984) Geological map of the Lusaka Area 1:250,000 sheet. Geological Survey of Zambia, Map No. SD-35–15
Thompson JB Jr (1981) An Introduction to the mineralogy and petrology of the biopyriboles. In: Veblen DR (ed) Amphiboles and other hydrous pyriboles – mineralogy. Mineralogical Society of America, Reviews in Mineralogy vol 9a, pp 141–188
Turner FJ, Weiss LE (1965) Deformational kinks in brucite and gypsum. Proc Nat Acad Sci 54:359–364
Vidale RJ (1974) Vein Assemblages and metamorphism in Dutchess County, New York. Geol Soc Am Bull 85 2:303–306
Vinyu ML, Hanson RE, Martin MW, Bowring SA, Jelsma HA, Krol MA, Dirks PHGM (1999) U–Pb and 40Ar/39Ar geochronological constraints on the tectonic evolution of the easternmost part of the Zambezi orogenic belt, northeast Zimbabwe. Precambrian Res 98:67–82
Vrana S, Prasad R, Fediuková E (1975) Metamorphic kyanite eclogites in the Lufilian Arc of Zambia. Contrib Mineral Petrol 51:139–160
Walther JV, Wood BJ (1984) Rate and mechanism in prograde metamorphism. Contrib Mineral Petrol 88:246–259

Waters DJ, Martin HN (1993) Geobarometry of phengite-bearing eclogites. Terra Abstr 5:410–411

Wayte GJ, Worden RH, Rubie DC, Droop GTR (1989) A TEM study of disequilibrium plagioclase breakdown at high pressure: the role of infiltrating fluid. Contrib Mineral Petrol 101:426–437

Widmer T, Thompson AB (2001) Local origin of high pressure vein material in eclogite facies rocks of the Zermatt-Saas zone, Switzerland. Am J Sci 301:627–656

Yuan X, Sobolev SV, Kind R, et al. (2000) Subduction and collision processes in the Central Andes constrained by converted seismic phases. Nature 408:958–961